Journal of Chemical Health Risks

www.jchr.org

JCHR (2023) 13(4), 1789-1797 | ISSN:2251-6727

# Synthesis of butyl propionate: A possible monomer for biodegradable polymer

**Kusuma Midathana, K.V. Ramesh, G.V.S. Sarma***
Department of Chemical Engineering, Andhra University, Visakhapatnam-530003, India.

**(Received: 02 September 2023 Revised: 14 October Accepted: 07 November)**

**KEYWORDS**

Bio-degradable, ester, fuel additive, reaction kinetics, thermodynamic model.

**Abstract**
As the earth passed out of global warming era and entering into the global boiling era, immediate preventive action is to be undertaken in this regard especially in the fields of energy and environment. The monomer butyl propionate acts as a fuel additive and its polymer has biodegradable nature. Hence butyl propionate provides one of the satisfactory answers for this problem. In the present work, the butyl propionate is synthesized by carrying out an esterification reaction from its constituent alcohol and acid and its kinetics have been evaluated. This reaction shows best performance in the presence of sulphuric acid catalyst. Under the range of variables investigated, no side reactions were observed as is evident from TLC, IR and NMR analyses. The reaction kinetics predicted from thermodynamic models was observed to be not satisfactory.

## Introduction

India has been making relentless efforts in developing and innovating new processes and technologies with an aim to meet the Sustainable Development Goals of United Nation's Envision 2030. Adopting green processes and technologies would obviously help in accomplishing these goals. Thus, the focus is mainly on conservation of energy and the environment. The butyl propionate, which is formed from small chain aliphatic alcohol i.e., butanol, is suitable as an additive to high-speed diesel and motor spirit. This in turn reduces the consumption of fossil fuels. Further, the polyesters that are produced from the butyl propionate are one of the biodegradable polymers. These polyesters are useful in many domestic, industrial, and commercial applications. The use of esters as insecticides and polyesters in the production of plastics is highly encouraged because of their biodegradable nature. The esters are also found to have wide applications in organic synthesis as intermediates and as well as finished products [2, 4, and 7]. As intermediates, the esters are important constituents in the manufacture of pharmaceuticals and fine organic chemicals. Many end products such as aspirin are also used as medicines. The esters as end products are useful as essential oils, fuel additives, medicines, and feed materials for a large number of industrial products. Therefore, the importance of esters in the process industry is of high magnitude and is indispensable. However, it is noticed that there are many lacunae in the concerned literature in esterification that require further investigations [6]. In this connection the present work is taken up. Propionic acid – n-butanol system is the chosen reacting system and the concerned reactions are given below:

$$\mathrm{CH_3CH_2COOH(l)} + \mathrm{CH_3(CH_2)_3OH(l)} \underset{}{\overset{H_2SO_4}{\rightleftharpoons}} \mathrm{CH_3CH_2COOCH_3(CH_2)_3(l)} + \mathrm{H_2O\ (l)} \ldots (1)$$

(Propionic acid) (n-Butanol) (Butyl Propionate) (water)

The present study essentially comprises determining the effect of temperature, mole ratio and catalyst concentration on conversion of acid. An effort is also made to know the existence of any side reactions. The suitability of thermodynamic models such as NRTL, UNIFAC and UNIQUAC is also examined in this work. Reaction rate constants are evaluated from the experimental data and correlation equations for these rate constants in terms of operating parameters are obtained by using least squares regression analysis.

**Experimental**

The apparatus used for the esterification reaction mainly consisted of a batch reactor, which is essentially a three-necked round flat-bottomed flask of 500 ml capacity, and a magnetic stirrer with a hot plate (Model No. Remi 5 MLH PLUS) which provides constant temperature and stirring speed. The temperature and the stirring speed of the magnetic stirrer were adjusted by using the heating knob and speed control knob. The set values for both temperature and stirrer speed could be read from the display of the magnetic stirrer. A reflux condenser was connected vertically at the center neck of the reaction flask for condensing the vapours of the reaction mixture. The thermocouple sensor was inserted into one of the side necks of the flask for precise temperature control. Normally, a stopper was used to close the other side neck and it was used whenever a sample needed to be taken out.

The experiments were performed at temperatures of 50°C, 60°C and 70°C; molar ratio of acid to alcohol of 0.5, 1.0 and 1.5; and catalyst concentrations of 1.0, 2.0 and 3.0 wt percent. A full factorial design for three independent variables was carried out. It is understood that the esterification reaction can be carried out either as a homogeneous reaction or as a heterogeneous reaction. For homogeneous reactions sulphuric acid or other acids are generally used as catalysts. Whereas for heterogeneous reactions, synthetic catalysts such as Amberlyst etc were used. However, the use of such synthesized catalysts yielded no economic advantage over sulphuric acid because of their high manufacture cost. Further the yield is also comparable. Hence, based on economic criterion, the use of sulphuric acid as a catalyst is advantageous [5].

**Results and discussion**

The reaction products are subjected to instrumental analysis to ascertain whether any byproducts formed or not. Thin Layer Chromatography (TLC), Infrared Spectroscopy (IR) and Nuclear Magnetic Resonance (NMR) spectroscopy have been used in the present study. Initially, the formation of product was confirmed using TLC technique without any by-product formation. This analysis was treated as the preliminary examination for the identification of product formation in the reaction mixture.

The IR spectrum obtained for the product butyl propionate has been shown in Fig.1. In the functional group region, the peak that is present and should be present is a sp3 C-H peak at 2850-3300 cm$^{-1}$. This peak is present in the IR spectrum at 2961.19 cm$^{-1}$. The carbonyl stretches C=O of aliphatic esters appear from 1680-1750 cm$^{-1}$. This peak is present at 1714.73 cm$^{-1}$ in the IR spectrum. A peak that is absent and should be absent from the IR spectrum is the O-H peak at around 3230-3550 cm$^{-1}$. There are no peaks in that region. A conclusion that can be drawn about the functional group region is that the starting material was converted into butyl propionate, since the product lacks an O-H peak and has a C-H peak, which shows a butyl group attached to an ester.

The fingerprint region occurs around the 1450-500 cm$^{-1}$ range. The C-O peak should also be present around 1000-1300 cm$^{-1}$, which indicates an ester. No peaks should be absent other than a combination of a C=O peak with an O-H peak should be absent, which indicates the presence of a carboxylic group. This peak is absent in the IR spectrum. There are no peaks present or absent that should not be. The lack of a C=O peak with an O-H peak and the presence of C=O peak and the C-O peak shows that an ester is present in the product and a carboxyl group is absent.

Please insert Fig.1 here.

Please insert Table 1 here.

The IR spectrum supports the synthesis of butyl propionate.The presence of an sp3 C-H peak and the absence of an O-H peak shows that the resulting product is butyl propionate, since it shows the lack of a carboxyl group. Additionally, the presence of C=O peak in functional group region and C-O peak in the fingerprint region shows that the product is ester. This concludes that the product must be butyl propionate. The IR spectrum also confirmed that the product is butyl propionate since it showed an ester peak and did not have an alcohol peak.

As seen in the $^{1}$H NMR spectrum of butyl propionate in Fig.2. the units of the abscissa in the spectrum in ppm and the signals stand at different positions along the x-axis. The height of the peak on the ordinate is proportional to the number of 1H nuclei in the molecule with the same chemical shift.

Please insert Fig.2 here

There are two different types of hydrogens present in esters. Hydrogens on the carbon attached to the oxygen (R-COO-CH$_2$-) are more deshielded due to the electronegativity of oxygen and they appear in the range 4-5 ppm. The other types of hydrogens are α-hydrogens

(R-$CH_2$-COOR) and they resonate in the range 2.1-2.5 ppm. These protons are deshielded by the anisotropy of the carbonyl (C=O) group. Again, all types of carbonyl functional groups give rise to NMR absorptions in the range 2.1-2.5 ppm due to α-hydrogens. Therefore, an ester group in a compound can be identified by the NMR absorptions in the 4-5 ppm region.

It is calculated by a simple equation to estimate the number of multiple bonds and rings. It assumes that oxygen (O) and sulfur (S) are ignored, and halogen (Cl, Br) and nitrogen is replaced by CH. The resulting empirical formula is CxHy.

Double Bond Equivalent (DBE) = [(2x + 2) – y]/2.

DBE of **$C_7H_{14}O_2$ = [(2*7+2)-14]/2= 1**

The DBE =1, and it is given that the compound is an ester, thus one double bond is accounted for –O-C=O (ester) group.

The influence of neighbouring groups (deshielding) on 1H chemical shifts is additive (to an extent). Shoolery's additivity rules for predicting the chemical shift of protons is given by:

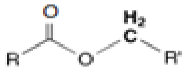

d (ppm) = 0.233 + S si

From the above spectrum, fragment (D) is located at 5.766 ppm which is 4–5 ppm from the literature. Here, in this spectrum the value of chemical shift is obtained as 5.766 ppm due to impurities present in the sample solution. Fragment (C), is located at 3.971 ppm. Fragment (B), R**$CH_2$**OR' is located at 2.205 ppm. From the spectrum, fragments E & F located at 1.123 ppm. And finally, the fragments A& G are located at 0.837 ppm. Hence, we can say that ester functional groups are identified. These details are compiled in Table 2.

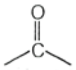

Please insert Table 2 here.

The 1H NMR shows a peak with a chemical shift around 6.0 ppm that has 1 proton and the peak at 3-4 ppm has 1.82 protons ~ 2 protons. Then, there seems to be a peak with 1.5 protons~ 2 protons at 2- 2.5 ppm. Lastly, the peak around 0.6-1.5 ppm has 8.57 protons ~ 9 protons.

Thus, there are a total of 1+2+2+9 = 14 protons which is consistent with the molecular formula provided. Altogether, the 1H NMR has 14 protons and the only product with 14 protons is butyl propionate.

**Effect of operating parameters**

The effect of the catalyst concentration on propionic acid conversion with time was studied at different mole ratios and temperatures. Fig. 3 shows the conversion of propionic acid with time during esterification with 1.0 and 3.0wt% of catalyst concentrations, the mole ratio of acid to alcohol and temperature being 1.0 and 50°C respectively. From this, it is evident that conversion increases with increasing catalyst concentration.

Please insert Fig.3 here

The effect of temperature on the reaction rate for propionic acid esterification with n-butanol was studied by conducting the reaction at three different temperatures 50, 60 and 70°C. The data presented in Fig.4. are at reaction condition of acid-to-alcohol ratio 1.5 and catalyst loading of 1.0wt%. The results indicated that conversion increased with an increase in the temperature.

Please insert Fig.4 here

The conversion of propionic acid with time is shown in Fig.5 for a catalyst concentration of 2.0 wt% and at a temperature of 70°C and for three mole ratios of viz., 0.5, 1.0 and 1.5. The conversion obtained was maximum in the case of 0.5 mole ratio.

Please insert Fig.5 here

**Interpretation of the kinetic data**

In general, a second order reversible can be written as:

$$\mathrm{A + B \rightleftarrows C + D} \qquad \ldots (2)$$

For the second- order reversible reaction the rate equation is:

$$-\mathrm{r_A} = -\frac{\mathrm{dC_A}}{\mathrm{dt}} = \mathrm{K_1\, C_A C_B - K_2 C_C C_D} \qquad \ldots (3)$$

**Case-1:** $C_{A0} = C_{B0}$, and $C_{C0} = C_{D0} = 0$

$$\ln\left[\frac{\mathrm{X_{Ae}-(2X_{Ae}-1)X_A}}{\mathrm{(X_{Ae}-X_A)}}\right] = 2\mathrm{K_1}\left(\frac{1}{\mathrm{(X_{Ae}}} - 1\right)\mathrm{C_{A0}t} \quad \ldots (4)$$

**Case-2:** $C_{A0} \neq C_{B0}$ and $C_{C0} = C_{D0} = 0$

Beula and Tsai [3] gave the following equation:

$$-\ln\frac{\{2X_A[(M+1)X_{Ae}-M]-[(M+1)X_{Ae}^2-X_{Ae}Z]\}\{(M+1)X_{Ae}^2 -}{\{2X_A[(M+1)X_{Ae}-M]-[(M+1)X_{Ae}^2+X_{Ae}Z]\}\{(M+1)X_{Ae}^2 -} = \frac{K_1 Z C_{A0} t}{X_{Ae}} \ldots (5)$$

Where

$$Z = \sqrt{[(M+1)^2 X_{Ae}^2 - 4M(MX_{Ae} + X_{Ae} - M)]} \qquad \ldots (6)$$

Y=

$$-\,ln\frac{\{2X_A[(M+1)X_{Ae}-M]-[(M+1)X_{Ae}^2-X_{Ae}Z]\}\{(M+1)X_{Ae}^2+X_{Ae}Z\}}{\{2X_A[(M+1)X_{Ae}-M]-[(M+1)X_{Ae}^2+X_{Ae}Z]\}\{(M+1)X_{Ae}^2-X_{Ae}Z\}} \quad \ldots (7)$$

Then $Y = \frac{K_1 Z C_{A0} t}{X_{Ae}}$… (8)

From the plots of Y vs t rate constant for the forward reaction $k_1$ is obtained. These graphs are shown in Figs.6, 7 and 8.

Please insert Fig.6 here.

Please insert Fig.7 here.

Please insert Fig.8 here.

From $k_1$, the rate constant for backward reaction $k_2$ is obtained using the following equations.

For case I: $k_2 = \frac{k_1(1-X_{Ae})^2}{{X_{Ae}}^2}$ ... (9)

For case-II: $k_2 = \frac{k_1(1-X_{Ae})(M-X_{Ae})}{{X_{Ae}}^2}$ … (10)

By regression analysis, the correlation equation obtained for $k_1$ and $k_2$ are

$k_1 = 191.7(MR)^{1.657}(CC)^{0.6335}e^{-2398/T}$ … (11)

Average deviation = 7.284 percent

Standard deviation = 9.777 percent

$k_2 = 0.1078 \times 10^{-03}(MR)^{0.7433}(CC)^{-0.1828}\,e^{2046/T}$ … (12)

Average deviation = 8.549 percent

Standard deviation = 9.740 percent

**Thermodynamic modeling**

For the present case, the thermodynamic equilibrium constant can be written as

$K_E = (\frac{C_C C_D}{C_A C_B})(\frac{\gamma_C \gamma_D}{\gamma_A \gamma_B})$ …. (13)

or $K_E = K_C K_\gamma$ …. (14)

Here $K_E$ = thermodynamic equilibrium rate constant = $\frac{k_1}{k_2}$

$K_C$ = concentration based rate constant = $\frac{C_C C_D}{C_A C_B}$

$K_\gamma$ = activity coefficient-based rate constant = $\frac{\gamma_C \gamma_D}{\gamma_A \gamma_B}$

Activity coefficient values for each case were computed using ASPEN PLUS software. The methodology was described in [1]. The comparison of experimental data and the data obtained from models such as Wilson, NRTL, UNIFAC and UNIQUAC were plotted and shown in Fig.9 for one set of experimental conditions.

Please insert Fig.9 here.

A close inspection of the plots of these figures reveals that, in all the cases the predicted conversions were less than the actual conversion. Further, the UNIQUAC method yielded better prediction compared to other models. The deviation from the actual values by different models has been found to be within ±25 percent. This indicates that there are no successful models available for the prediction of esterification reaction and hence one has to depend on experiment for accurate data.

## Conclusions

Within the range of our study, there are no side reactions. This is evident from analyses made from TLC, FTIR and NMR spectroscopy. The conversion increased with an increase in mole ratio for all the reactions employed in the present study. With increase in catalyst concentration, the conversion also increased. With the increase in temperature the conversion increased.

## References

1. Al-Malah K.I.M.., Aspen Plus: Chemical Engineering Applications, Wiley, **(2016)**
2. Bart H.J., Kaltenbrunner W., & Landschützer H., Kinetics of esterification of acetic acid with propyl alcohol by heterogeneous catalysis, International Journal of Chemical Kinetics, **28(9)**, 649-656**(1996)**
3. Beula C., & Sai P. S. T., Kinetics of esterification of acetic acid and ethanol with a homogeneous acid catalyst, Indian Chemical Engineer, **57(2)**, 177-196**(2015)**
4. Kastratović V.R., Radulović M.M., & Kastratović K.K., Esterification of propanoic acid in the presence of a homogeneous catalyst, Kragujevac Journal of Science, **44**, 45-55**(2022)**
5. Kusuma M., Formation of propionates: Kinetics and thermodynamics, Ph.D. thesis, Andhra University, Visakhapatnam, India, **(2023)**
6. Otera J., & Nishikido J., Esterification, 2/e, Wiley-VCH, Weinheim, Germany, **(2010)**
7. Ramesh K. V., & Veerabhadra Rao K., Kinetic Studies of Esterification Using Response Surface Methodology (System: Iso-Propanol-Formic Acid), The Icfai University Journal of Chemistry, **2(1)**, 18-35**(2009)**

Table 1. Readings from IR spectrum shown in Fig.1.

| Functional Group | Characteristic Absorptions (cm $^{-1}$) | Intensity |
|---|---|---|
| C-H | 2961.19 | Stretch |
| C=O | 1714.73 | Stretch |
| C-C-O | 1187.44 | Stretch |
| O-C-C | 1073.09 | Stretch |

Table 2. Chemical shift values

| Assign. | Chemical shift values calculated from Shoolery's additivity rulesδ(ppm) | Chemical shift values (from the spectrum) | Neighbor H's | Multiplicity | Integration |
|---|---|---|---|---|---|
| A | 0.73 | 0.837 | 2 | triplet | 3 |
| B | 2.253 | 2.205 | 3 | quartet | 2 |
| C | 3.933 | 3.971 | - | - | - |
| D | 3.833 | 5.766 | 2 | triplet | 2 |
| E | 1.173 | 1.123 | 4 | pentet | 2 |
| F | 1.173 | 1.123 | 2+3 | multiplet | 2 |
| G | 0.73 | 0.837 | 2 | triplet | 3 |

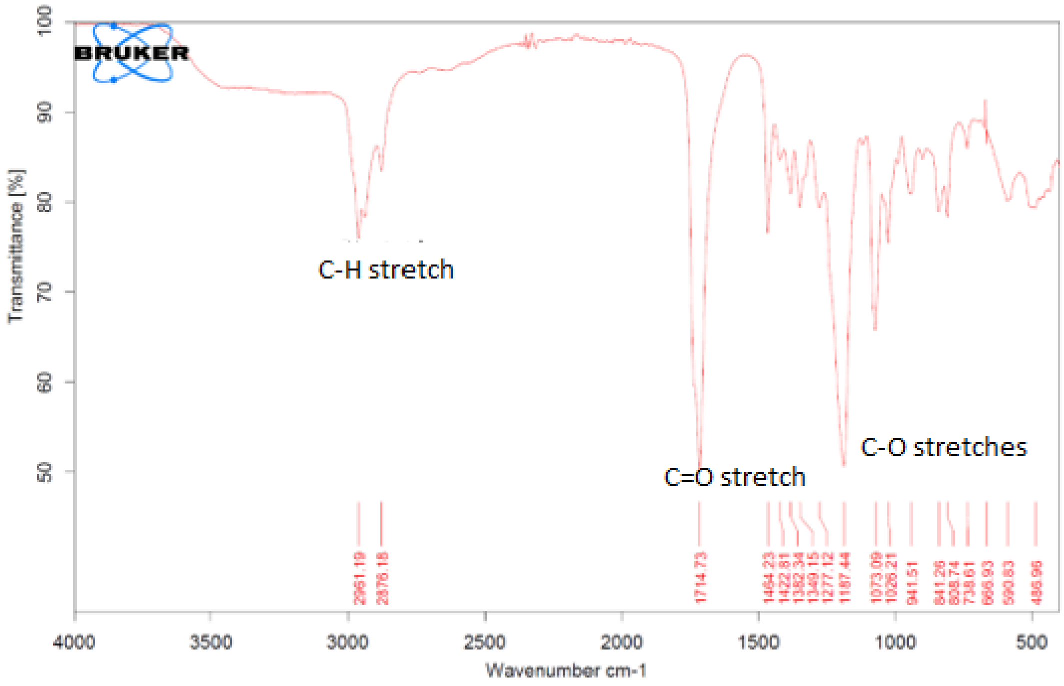

Fig. 1. IR spectrum for Butyl Propionate

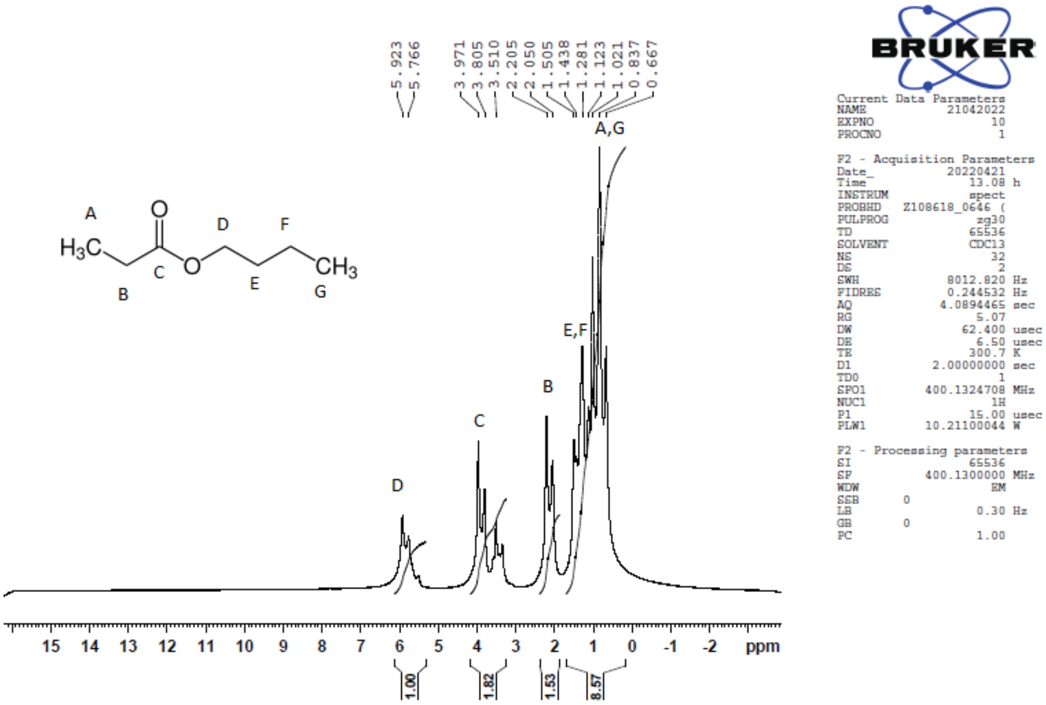

```
Current Data Parameters
NAME            21042022
EXPNO                 10
PROCNO                 1

F2 - Acquisition Parameters
Date_           20220421
Time               13.08 h
INSTRUM            spect
PROBHD   Z108618_0646 (
PULPROG             zg30
TD                 65536
SOLVENT            CDCl3
NS                    32
DS                     2
SWH             8012.820 Hz
FIDRES          0.244532 Hz
AQ             4.0894465 sec
RG                  5.07
DW                62.400 usec
DE                  6.50 usec
TE                 300.7 K
D1            2.00000000 sec
TD0                    1
SFO1         400.1324708 MHz
NUC1                  1H
P1                 15.00 usec
PLW1         10.21100044 W

F2 - Processing parameters
SI                 65536
SF           400.1300000 MHz
WDW                   EM
SSB      0
LB                  0.30 Hz
GB       0
PC                  1.00
```

Fig.2. $^1$H NMR for Butyl Propionate

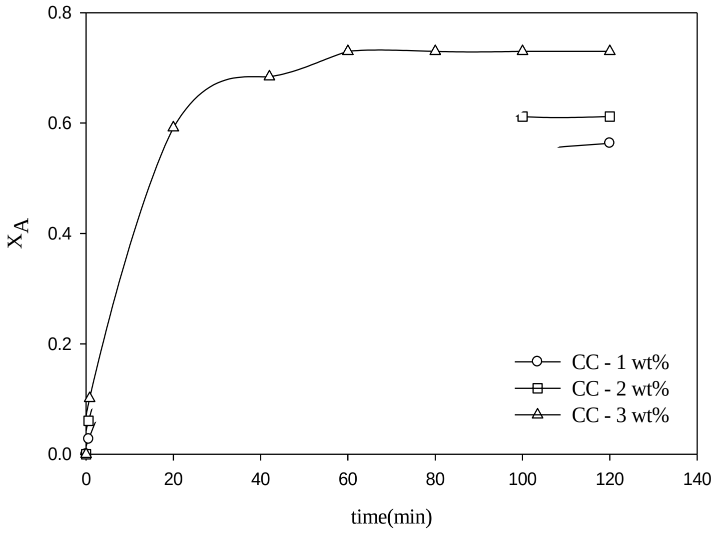

Fig.3. Effect of catalyst concentration on conversion { M.R = 1.0; T = 50°C }

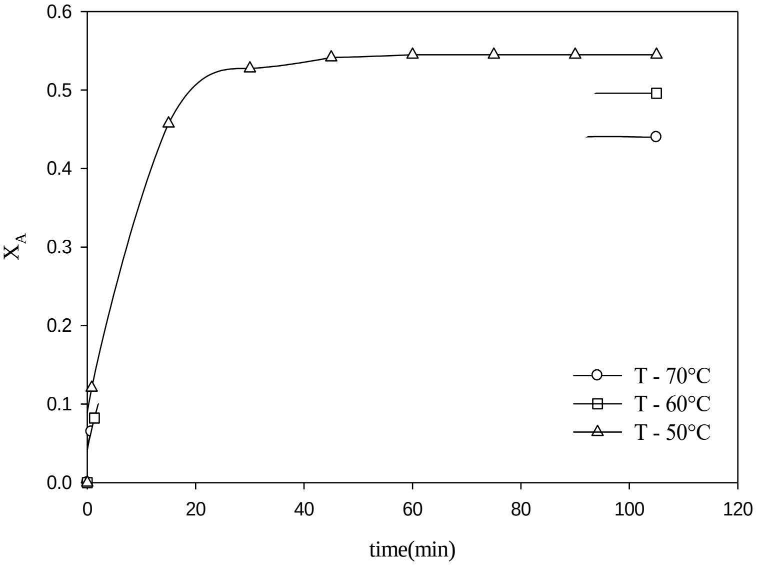

Fig.4. Effect of temperature on conversion { M.R = 1.5; C.C = 1.0 wt% }

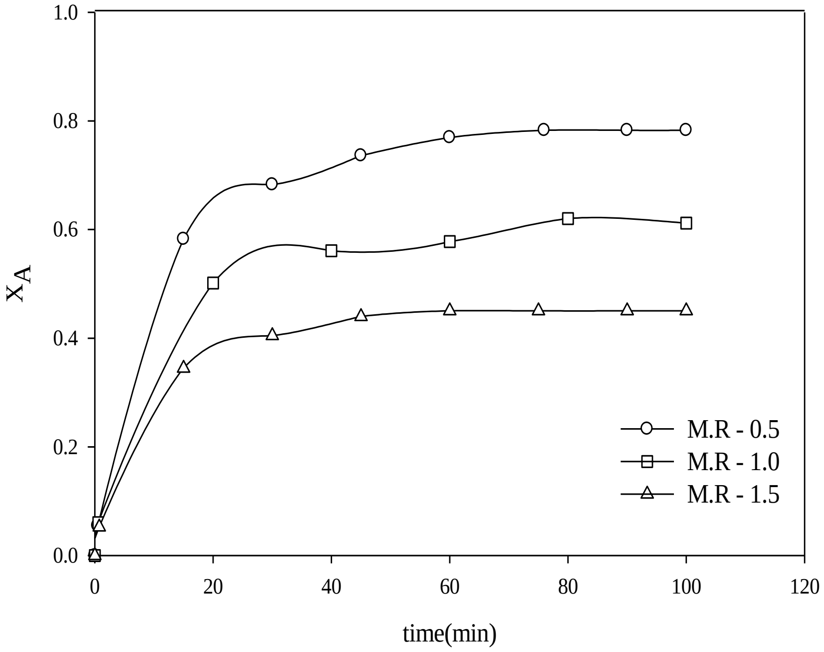

Fig.5. Effect of mole ratio on conversion { T = 50°C; C.C = 2.0 wt% }

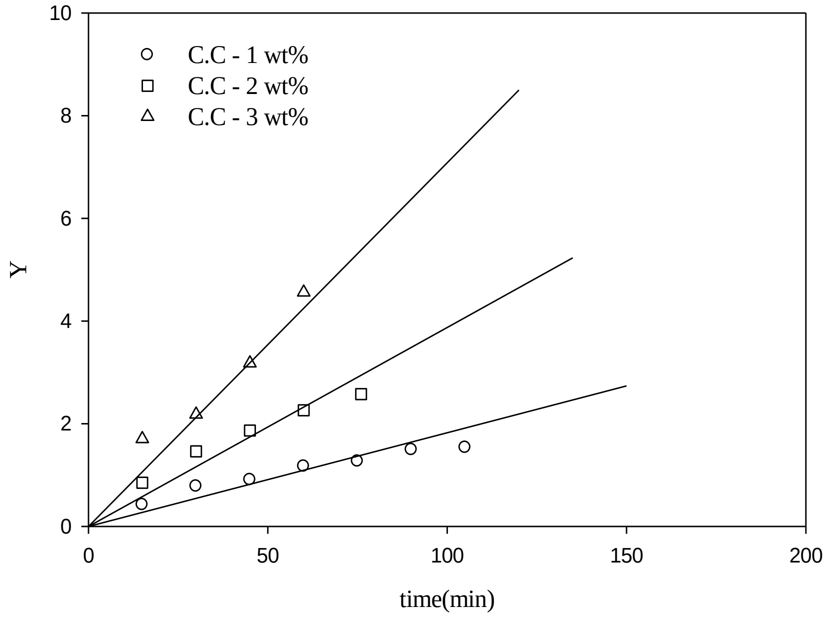

Fig.6. Test of the rate equation {M.R = 0.5; T = 50°C }

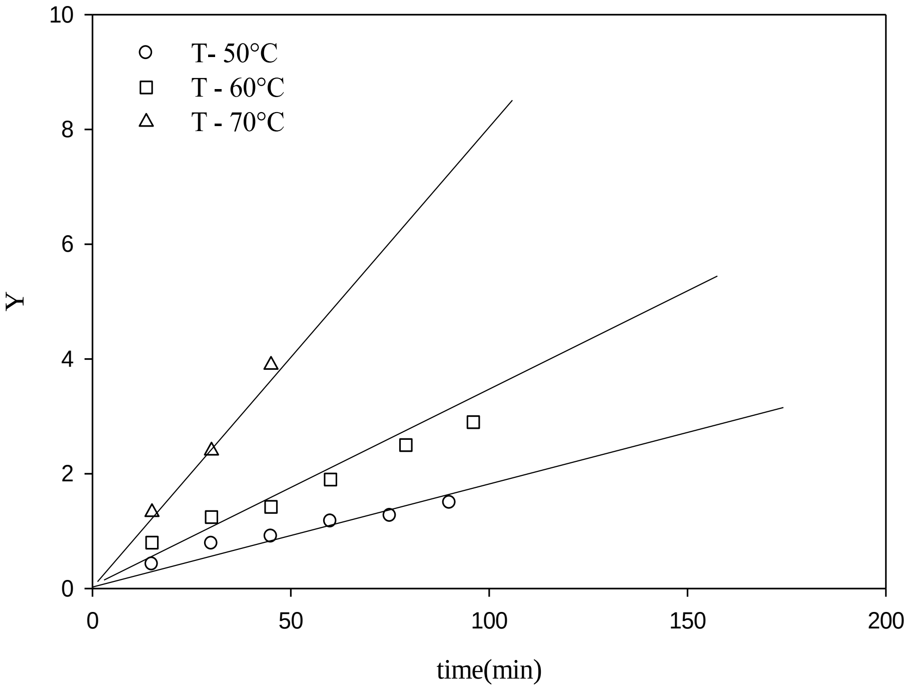

Fig.7.Test of the rate equation {M.R = 0.5; CC = 1.0 wt% }

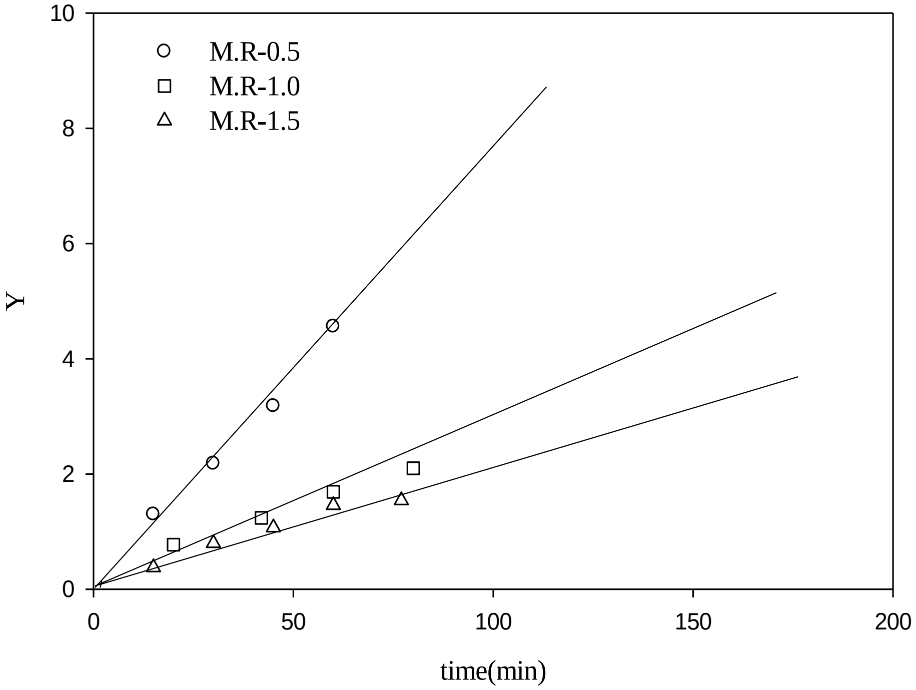

Fig.8. Test of the rate equation { T = 50°C; CC = 3.0 wt% }

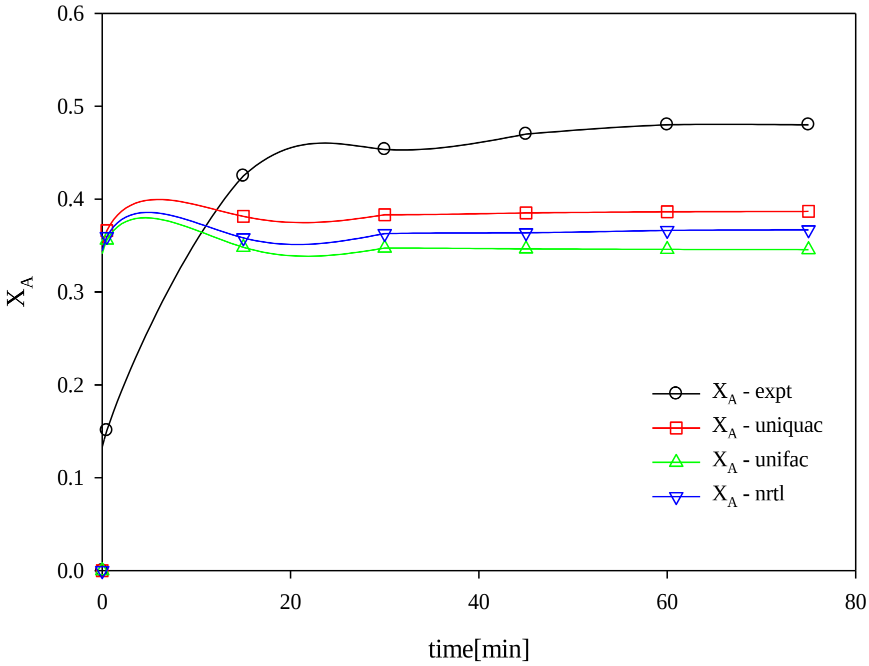

Fig.9. Concentration-based model fit {M.R =1.5; T = 70°C; CC = 3.0 wt%}